Environmental Science & Technology Letters

Letter

Cite This: Environ. Sci. Technol. Lett. 2018, 5, 302−308

pubs.acs.org/journal/estlcu

Source Apportionment of Brown Carbon Absorption by Coupling Ultraviolet−Visible Spectroscopy with Aerosol Mass Spectrometry

Vaios Moschos,[†,‡] Nivedita K. Kumar,[†,§] Kaspar R. Daellenbach,[†,∥] Urs Baltensperger,[†] André S. H. Prévôt,*[,†] and Imad El Haddad*[,†]

[†]Paul Scherrer Institute, Laboratory of Atmospheric Chemistry, CH-5232 Villigen-PSI, Switzerland

[‡]ETH Zurich, Department of Mechanical and Process Engineering, CH-8092 Zurich, Switzerland

Supporting Information

ABSTRACT: The impact of brown carbon (BrC) on climate has been widely acknowledged but remains uncertain, because either its contribution to absorption is being ignored in most climate models or the associated mixed emission sources and atmospheric lifetime are not accounted for. In this work, we propose positive matrix factorization as a framework to apportion the contributions of individual primary and secondary organic aerosol (OA) source components of BrC absorption, by combining long-term aerosol mass spectrometry (AMS) data with concurrent ultraviolet−visible (UV-vis) spectroscopy measurements. The former feature time-dependent factor contributions to OA mass, and the latter consist of wavelength-dependent absorption coefficients. Using this approach for a full-year case study, we estimate for the first time the mass absorption efficiency (MAE) of major light-absorbing water-soluble OA components in the atmosphere. We show that secondary biogenic OA contributes negligibly to absorption despite dominating the mass concentration in the summer. In contrast, primary and secondary wood burning emissions are highly absorbing up to 500 nm. The approach allowed us to constrain their MAE within a confined range consistent with previous laboratory work, which can be used in climate models to estimate the impact of BrC from these emissions on the overall absorption.

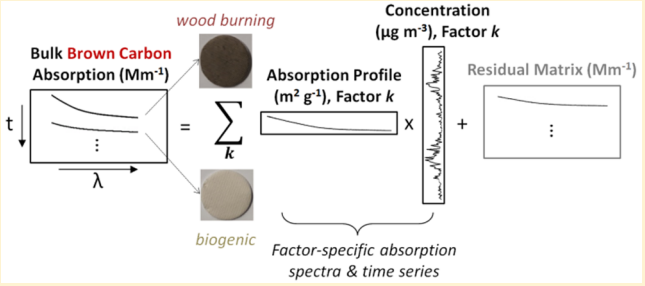

INTRODUCTION

The optical properties and sources of ambient particulate matter (PM) are of prime importance in the context of a changing climate.[1−3] Typically, organic aerosol (OA) contributes to 20−70% of PM, of which 40−80% is water-soluble (WSOA).[4] WSOA has recently been shown to contain light-absorbing compounds termed brown carbon (BrC).[5−7] Current estimates suggest that flaming and smoldering combustion of biomass emits ∼6.9 Tg of primary BrC per year,[8] while the oxidation of biogenic and anthropogenic precursors contributes to more than 5.7 Tg of secondary BrC per year.[8−13]

Soot (or black) carbon (BC) is a strong light absorber in both the ultraviolet (UV) and visible (vis) regions,[14] with a relatively constant wavelength dependence of absorption.[15−17] Although BC absorption is predominant in the visible region, the strongest output range of the Sun's total irradiance,[18] enhanced BrC absorption in this region has been observed[19] for OA heavily impacted by biomass burning, likely because of the presence of interacting functionalized polyaromatic moieties forming charge transfer complexes.[20] Recent research has revealed that BrC may contribute up to 15% to light absorption over the entire UV−vis spectrum[21,22] and up to 50% at shorter wavelengths.[22−24] This fraction affects tropospheric chemistry[25] and ground-level ozone concentrations[8] and can lead to perturbation of the Earth's radiative balance.[26] However, its main sources and optical properties, e.g., wavelength-dependent mass absorption efficiency (MAE), remain poorly constrained.

The bulk optical absorption properties of BrC have been characterized by UV−vis spectroscopy using liquid extracts.[27−31] This technique provides high spectral resolution[31] and wide spatial coverage, without interference from BC absorption, and allows for fast analysis of long-term absorption trends. However, current ambient studies of BrC are largely limited to correlations of the measured absorption with seasonal/diurnal patterns and specific marker species[10,30,32] or source apportionment model outputs.[16] While receptor models have been successfully utilized to apportion OA to specific primary emissions or formation processes,[33−39] the relationship between these OA sources and the associated OA absorptivity remains poorly defined,[40] hindering the quantification of the impact of these sources on climate.

In this letter, we introduce a novel approach to estimate component-specific BrC absorption properties for OA classes ubiquitous in the atmosphere. The approach uses a positive matrix factorization (PMF) model to combine long-term factor-

Received: March 7, 2018
Revised: May 8, 2018
Accepted: May 11, 2018
Published: May 11, 2018

DOI: 10.1021/acs.estlett.8b00118
Environ. Sci. Technol. Lett. 2018, 5, 302−308

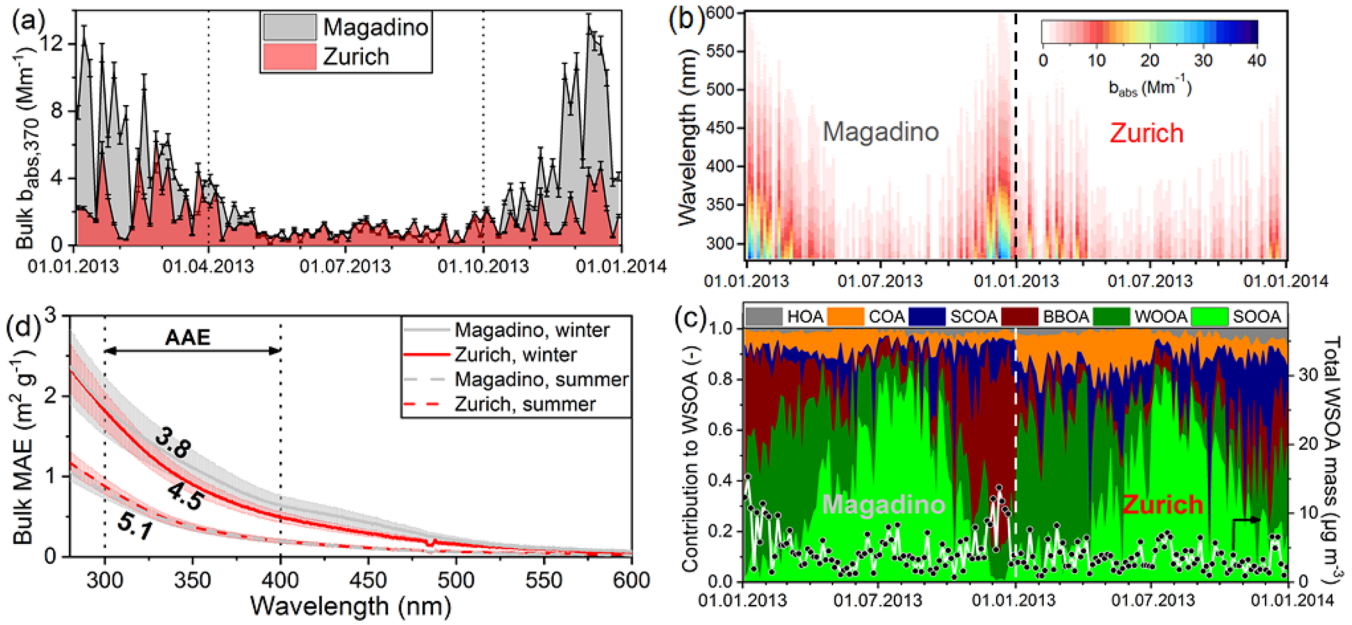

Figure 1. (a) Year-long time series of the bulk absorption coefficient at 370 nm, $b_{abs,370}$, of the light-absorbing organic (brown) carbon (BrC), estimated (eq S1) by UV−vis analysis (Text S2) of water-extracted ambient PM_{10} samples (Text S1) for Magadino (light gray) and Zurich (red). The error bars represent the 1σ error (eq S4, 68% confidence interval). (b) Image plot of the time- and wavelength-dependent bulk b_{abs} used as PMF input (matrix **X**, eq 1). (c) Water-soluble organic aerosol (WSOA) source components identified by AMS−PMF analysis (WSOC-based)[38] and their daily cumulative relative contributions (left *y*-axis) to the total WSOA mass (right *y*-axis) at both sites. These contributions are used to obtain the normalized OA factor time series (matrix **G**) used as model constraints (Figure S2). (d) Seasonally averaged (winter, summer) bulk mass absorption efficiency (MAE_λ, eq S2), where the wavelength dependence of the absorption is linked to sources by the average absorption Ångström exponent (AAE, eq S3).

specific WSOA mass concentrations obtained by offline aerosol mass spectrometry (AMS) and concurrent wavelength-dependent bulk absorption coefficients obtained by UV−vis spectroscopy. The resulting MAE spectra of major components are compared with those of reference BrC sources from controlled laboratory experiments and real-world aerosol samples. We conclude with comments about the general applicability of the introduced methodology, the aim being a deepened understanding of BrC climate effects.

MATERIALS AND METHODS

Aerosol Sampling and Analysis. Year-long ambient PM_{10} filter sampling was performed at two sites in Switzerland with different exposure characteristics: a rural alpine valley site in Magadino and an urban background site in Zurich. In addition, filters were collected from a tunnel in Switzerland and cooking oil heating experiments were performed to approximate the absorptivity of traffic- and cooking-related primary OA, respectively (Text S1).

The BrC absorption was recorded (Text S2) using a UV−vis spectrophotometer coupled to a liquid waveguide capillary cell.[28] The measured wavelength-dependent attenuation of the liquid extracts was converted (eq S1) to the blank-subtracted absorption coefficient, $b_{abs,\lambda}$ (in Mm^{-1}),[10,30,31] which was further used to calculate (eq S2) the bulk MAE (in m^2 g^{-1}). The average absorption Ångström exponent (AAE) was calculated (eq S3) in the range of 300−400 nm (step, 5 nm) to characterize BrC originating from various sources.[10,19,28,30,41]

AMS-based source apportionment was performed for Magadino and Zurich using filter water extracts.[38] Four primary and two secondary organic aerosol components were identified. These were hydrocarbon-like (HOA), cooking-related (COA), sulfur-containing (SCOA), and biomass burning (BBOA) and winter-oxygenated (WOOA) and summer-oxygenated (SOOA), respectively.

Determination of Component-Specific MAE. The measured absorption coefficient, $b_{abs,i,j}$ (*i*, sample date; *j*, wavelength, in Mm^{-1}), can be expressed as factor time series of WSOA mass concentration, $WSOA_{i,k}$ (in μg m^{-3}), times $MAE_{k,j}$ (in m^2 g^{-1}). We solve this equation using positive matrix factorization (PMF). This bilinear receptor model represents (eq 1) a matrix of time series (*i* time points) of measured quantities (*j* variables), $\mathbf{X}_{i,j}$, as a linear combination of *k* factor profiles, $\mathbf{F}_{k,j}$, and their time-dependent intensities, $\mathbf{G}_{i,k}$, where factors represent unique sources and/or processes.[42]

$$\mathbf{X}_{i,j} = \mathbf{G}_{i,k}\cdot\mathbf{F}_{k,j} + \mathbf{E}_{i,j} \quad (1)$$

Here, **X** contains 182 time points (91 per site per year) of the b_{abs} measured in the range of 280−600 nm. This formulation assumes volume additivity for the different components. The main advantage of this model over other linear models (e.g., multilinear regression and partial least-squares analysis) is the positive constraints on the elements of WSOA concentrations and MAE values. The model includes a matrix **E** of model residuals corresponding to **X**. To solve eq 1, an error matrix, $\mathbf{S}_{i,j}$ (eq S4 and Figure S1), is required to minimize an objective function *Q* through a least-squares process: $Q = \sum_i\sum_j(\mathbf{E}_{i,j}/\mathbf{S}_{i,j})^2$.

PMF is solved using the multilinear engine (ME-2) with the PSI Source Finder (SoFi) front/back end,[42,43] which improves factor resolution by extensive exploration of the rotational ambiguity, i.e., multiple solutions (**G**, **F** pairs) having similar *Q* values, including directing the solution toward environmentally meaningful rotations.[44] Here, the model was set up by constraining the elements of **G** to the normalized WSOA

DOI: 10.1021/acs.estlett.8b00118
Environ. Sci. Technol. Lett. 2018, 5, 302−308

factor time series [dimensionless (Figure S2)] such that the obtained **F** would denote the yearly average absorption coefficient for each factor at various wavelengths, upon normalization by the total number of samples. Each element of **G** was constrained within a predetermined range representing the uncertainties obtained from ref 38. Dividing **F** by the yearly WSOA concentration of the respective factors, we can obtain the $MAE_{k,j}$ matrix. We note that following this setting, the factor contributions to bulk BrC absorption would be independent of the absolute values of the $WSOA_{i,k}$ concentrations, while the $MAE_{k,j}$ matrix elements depend on these absolute concentrations.

The confidence interval on the retrieved absorption spectra was assessed using a classical bootstrap approach.[36,37,44] This is based on the creation of replicate data sets by resampling the original data through random resampling of the rows of **X**. For each bootstrap run, the values of **G** were modified by selecting different solutions provided by Daellenbach et al.[38] In addition, the effect of blank subtraction on the $b_{abs,i,j}$ values was assessed by modifying the blank spectrum within its variability.

RESULTS AND DISCUSSION

UV−Vis Absorption. Figure 1a shows the absorption coefficient at 370 nm, $b_{abs,370}$, in Magadino and Zurich over a yearly cycle. Figure 1b shows the absorption coefficients at all wavelengths, used as PMF model input (matrix **X**, eq 1). A seasonal trend in the absorption at both sites and all wavelengths can be clearly observed, with higher absorption in winter months, particularly in Magadino where biomass burning activity is more intense (Figure 1c, BBOA). The wintertime $b_{abs,370}$ is 5.6 ± 3.7 Mm^{-1} in Magadino and 2.2 ± 1.6 Mm^{-1} in Zurich. The absorption drops to 1.0 ± 0.7 Mm^{-1} at both sites during summer, when summer-oxygenated OA (SOOA) is predominant in terms of mass (Figure 1c).

The bulk MAE_{370} in Switzerland averages ∼0.9 and 0.28 $m^2\ g^{-1}$ during winter and summer, respectively (Figure 1d). A similarly high MAE_{365} (1.22 ± 0.11 $m^2\ g^{-1}$) was reported in Beijing during winter,[30] where biomass and coal burning are important OA sources. Such higher MAE values indicate that stronger light-absorbing organic compounds might originate from biomass burning than from other sources, in line with previous studies.[28,29] This statement is further supported[19] by the lower AAE values observed in winter (<4.5) versus summer (∼5.1) in the seasonally averaged absorption spectra, with an extended absorption toward visible wavelengths[24] in Magadino during winter. The higher absorption efficiency of biomass smoke is likely related to the presence of polar aromatic compounds within this source,[20,45] potentially associated with phenolic species from lignin pyrolysis.[46]

Model Setup. For the source apportionment model, we have considered only BBOA, WOOA, and SOOA, as the absorption by the other factors was estimated to be negligible (Text S3 and Figure S3). The three-factor solution is validated by the excellent accuracy and sufficient model precision (Figure S4). Model errors are consistent throughout the year at both sites with an average of ∼40%, of which ∼25% can be attributed to measurement errors. The remainder is most likely related to the day-to-day variability of the component-specific absorption profiles. We further demonstrate that test models considering that (1) all factors absorb equally (Figure S5) or (2) only BBOA is absorptive (Figure S6) cannot capture the observed absorption variability. The relative bias (Figures S5 and S6) and scaled residuals (Figure S7) for both test models exhibit a clear spatial and temporal pattern. Model 1 underestimates (overestimates) significantly the absorption in winter (summer), while model 2 clearly overestimates (underestimates) the absorption at high BBOA (high WOOA) concentrations.

An unconstrained model, without including AMS data, was also examined (Figure S8). This model was able to separate the contribution of primary BBOA to total absorption from the sum of the secondary OOA factors, providing compelling evidence that the different aerosol components exhibit specific absorption features that allow their distinction by PMF. The model results are comparable to those presented here, when the contributions of both OOA factors to absorption are combined. This indicates that the constrained model using the mass concentration time series of the aerosol fractions obtained by AMS is capable of faithfully reproducing the variability in the absorption measurements. However, the unconstrained model could not separate the contributions of the two OOA factors, likely because of the low SOOA absorption. In addition, such a setting inherently hinders the provision of a direct link of the retrieved absorption spectra to specific sources and/or processes and renders any intended quantitative estimation of the factor-specific MAE spectra challenging. Finally, the results were heavily dependent on the pseudorandom starting point of the model (unstable output), indicating the need for using constraints.

Model Results. Figure 2 shows the modeled yearly average $b_{abs,\lambda}$ for the three WSOA components. Primary biomass

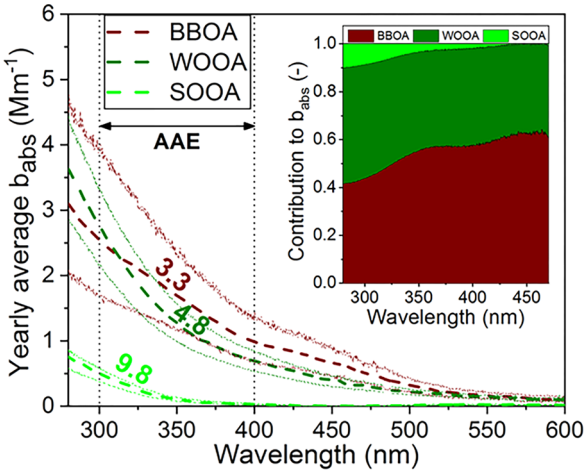

Figure 2. Yearly average $b_{abs,\lambda}$ apportioned to three WSOA components (thin lines, 10th and 90th percentiles) using output matrix **F** (eq 1), along with the associated factor-specific average AAE values. The inset shows the yearly wavelength-dependent cumulative relative factor contributions to the total BrC absorption at both sites.

burning, from wintertime residential combustion,[47,48] is the most absorbing water-soluble component with MAE values at 370 nm of 1.37 (0.99−1.91) $m^2\ g^{-1}$ (Figure S9). Its absorption extends to the visible range with a clearly visible hump between 400 and 470 nm (MAE ∼ 0.76 $m^2\ g^{-1}$). The lower BBOA AAE of 3.3 compared to the other factors reflects the significant contribution of BBOA to absorption during winter (Figure 1d). This contribution averages 55% on an annual basis (Figure 2, inset), with an increasing trend toward longer wavelengths (daily factor contributions to total absorption shown in Figure S10).

DOI: 10.1021/acs.estlett.8b00118
Environ. Sci. Technol. Lett. 2018, 5, 302−308

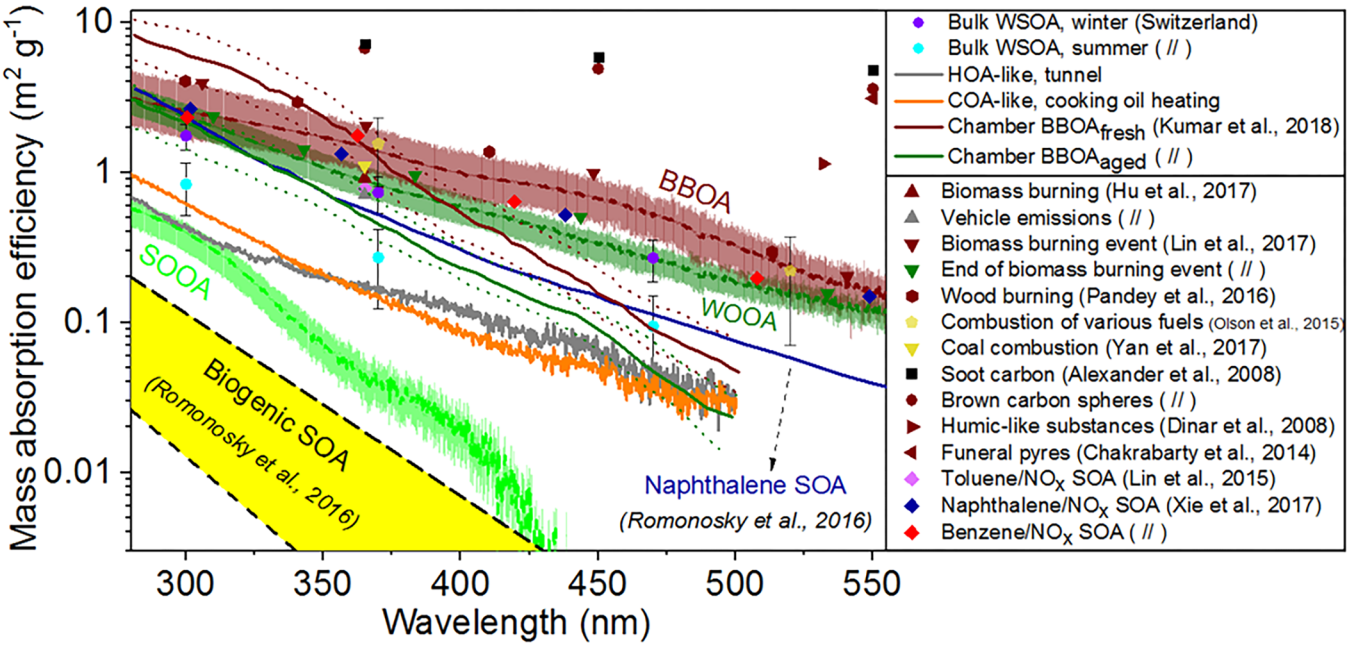

Figure 3. Comparison of the modeled mass absorption efficiency (MAE) spectra (Figure S9) to those of primary and aged wood burning BrC from chamber experiments (dotted lines, first and third quartiles), field-collected mixed-source samples, and laboratory experiments employing anthropogenic and biogenic SOA precursors (average values shown here). The MAE spectra of the methanol-soluble HOA-like (gray) and average COA-like (orange) components excluded from PMF analysis (Text S3) are included in the same graph.

The retrieved BBOA MAE values follow reported values (Figure 3) of extracted ambient samples with a strong biomass burning influence[49,50] and from laboratory tests of open and residential combustion of various fuels.[51−54] It is noteworthy that direct coal emissions from residential heating[54] have an MAE similar to that of BBOA, implying that residential sources are likely to influence the total absorption through BrC emissions, at locations where either coal or biomass burning is important. By contrast, the MAE values determined here are lower than those of nonconventional BrC types, such as amorphous BrC spheres,[55] humic-like substances,[56] and funeral pyres.[57] While these components may be present in primary biomass smoke, they most likely coexist with weakly absorbing matter, e.g., anhydrous sugars from cellulose pyrolysis, which lowers the bulk absorption efficiency.

WOOA largely consists of highly oxidized OA from nonfossil origins, correlates with anthropogenic secondary inorganic species, and peaks during transport events from continental Europe, which suggests that this component is likely associated with the oxidation of primary aerosols or gas-phase precursors present in biomass smoke.[38,39,58,59] The absorption efficiency of WOOA equals 0.81 (0.63−0.99) $m^2\ g^{-1}$ at 370 nm and is lower than that of primary biomass smoke, although not statistically significantly at all wavelengths. While aging of biomass smoke may produce additional absorbing matter that enhances the bulk absorption coefficient,[53] the lower MAE of aged biomass smoke compared to that of primary emissions is consistent with recent results.[49,60] The WOOA absorption profile is remarkably similar to that of SOA from common anthropogenic precursors,[12,13,61] consistent with the hypothesized origin of this component.[62,63] However, WOOA seems to be more absorbing than the chamber-generated aged BBOA,[53] indicating the influence of processes that are not yet accounted for in the latter case.

The temperature-driven nonfossil SOOA, which constitutes the most important WSOA source in the summer, is expected to largely originate from biogenic volatile organic compounds.[38,39] The difference in the composition and origins between SOOA and WOOA is clearly reflected in their dramatically different absorption properties. The MAE of SOOA is ∼0.04 $m^2\ g^{-1}$ at 370 nm, 20 times lower than that of WOOA. Unlike the other two components, SOOA absorbs only in the UV range, contributing on average to 7% of the absorption below 350 nm on an annual basis (Figure 2, inset). At longer wavelengths, the SOOA MAE values are highly uncertain (factor of >2). We note that the SOOA MAE_λ is higher than that determined in chambers for SOA from O_3- and OH-initiated oxidation of various biogenic precursors[61] (e.g., limonene and α-pinene). This points to additional unknown sources (e.g., oxidation of fossil precursors[59,64]) or formation mechanisms[65] (e.g., NO_3-initiated oxidation of terpenes, intraparticle reactions, or interactions between anthropogenic and biogenic emissions) of summertime BrC.

Perspective. We provide a unique framework for the determination of key optical absorption properties of individual OA source components, by deconvolving the long-term water-soluble brown carbon absorption of real-world mixed-source samples. This novel platform may be applied to other data sets, including environments that are heavily polluted[66] or largely represented by other sources (e.g., coal combustion in China[54]). The approach may also be suited for online data sets, acquired using aerosol mass spectrometry and various online optical measurement techniques, to provide insights into non-extractable OA fractions.[67] The model results are expected to be sensitive to the applied mass spectrometric analysis, including factor separation criteria, uncertainty estimation, type of employed mass spectrometer, and time resolution (Text S3). Such sensitivity has to be assessed in similar future studies.

The proof-of-concept application of this technique in this work provided the first estimation of the mass absorption efficiency of three major water-soluble OA sources: primary biomass smoke, aged biomass smoke, and biogenic secondary

DOI: 10.1021/acs.estlett.8b00118
Environ. Sci. Technol. Lett. 2018, 5, 302−308

OA. We show that under conditions representative of central European aerosols,[68] primary and secondary biomass burning emissions dominate the OA absorption despite the large contribution of biogenic emissions to OA mass. The MAE constrained in this study can be used to predict the impact of the water-soluble fraction of these emission sources on climate, through Mie calculations and radiative transfer modeling.

■ ASSOCIATED CONTENT

Supporting Information

The Supporting Information is available free of charge on the ACS Publications website at DOI: 10.1021/acs.estlett.8b00118.

Details regarding aerosol sampling (Text S1), UV−vis spectroscopy measurements and analysis (Text S2), AMS-resolved components and factor selection for PMF analysis (Text S3), error model validation (Figure S1), normalized time series of the mass concentration for each selected factor (Figure S2), an indication of the negligible absorption of the SCOA component (Figure S3), correlation between modeled and measured bulk absorption coefficients for the three combined (Figure S4), one combined (Figure S5), and one-factor (Figure S6) test models along with the respective time series of the scaled residuals (Figure S7), unconstrained test model results (Figure S8), retrieved factor-specific MAE spectra (Figure S9), and time series of the wavelength-dependent relative factor contributions to bulk absorption (Figure S10) (PDF)

■ AUTHOR INFORMATION

Corresponding Authors

*E-mail: imad.el-haddad@psi.ch.
*E-mail: andre.prevot@psi.ch.

ORCID

Vaios Moschos: 0000-0002-6251-4117

Present Addresses

[§]N.K.K.: Oceaneering Asset Integrity, 7052 Trondheim, Norway.
[∥]K.R.D.: University of Helsinki, Institute for Atmospheric and Earth System Research, FI-00014 Helsinki, Finland.

Author Contributions

V.M. contributed to project design, performed the UV−vis measurements, led the data analysis, prepared the figures, and wrote the manuscript. N.K.K. contributed to project design and data analysis and discussed the results. K.R.D. provided the mass spectrometric data and discussed the results. U.B. supervised the work and revised the manuscript. A.S.H.P. contributed to project design, supervised the work, and aided with data interpretation. I.E.H. led the project design and supervision and contributed to data analysis and the preparation of the figures and the manuscript.

Notes

The authors declare no competing financial interest.

■ ACKNOWLEDGMENTS

This work has been supported by funding from the European Union's Horizon 2020 research and innovation programme under Grant 689443 via project ERA-PLANET (The European network for observing our changing planet), and the Swiss Federal Office for the Environment (FOEN). V.M. acknowledges the Onassis Foundation (Greece) for a graduate student scholarship. The authors thank Jay G. Slowik for fruitful discussions, Athanasia Vlachou for computational assistance, AWEL Zurich for providing the tunnel samples, and six anonymous reviewers for their positive feedback and constructive comments on the submitted manuscript.

■ REFERENCES

(1) Pöschl, U. Atmospheric aerosols: Composition, transformation, climate and health effects. *Angew. Chem., Int. Ed.* **2005**, *44*, 7520−7540.
(2) Kanakidou, M.; Seinfeld, J. H.; Pandis, S. N.; Barnes, I.; Dentener, F. J.; Facchini, M. C.; Van Dingenen, R.; Ervens, B.; Nenes, A.; Nielsen, C. J.; et al. Organic aerosol and global climate modelling: a review. *Atmos. Chem. Phys.* **2005**, *5*, 1053−1123.
(3) Bahadur, R.; Praveen, P. S.; Xu, Y.; Ramanathan, V. Solar absorption by elemental and brown carbon determined from spectral observations. *Proc. Natl. Acad. Sci. U. S. A.* **2012**, *109*, 17366−17371.
(4) Jaffrezo, J.-L.; Aymoz, G.; Delaval, C.; Cozic, J. Seasonal variations of the water soluble organic carbon mass fraction of aerosol in two valleys of the French Alps. *Atmos. Chem. Phys.* **2005**, *5*, 2809−2821.
(5) Andreae, M. O.; Gelencsér, A. Black carbon or brown carbon? The nature of light-absorbing carbonaceous aerosols. *Atmos. Chem. Phys.* **2006**, *6*, 3131−3148.
(6) Kirillova, E. N.; Andersson, A.; Han, J.; Lee, M.; Gustafsson, Ö. Sources and light absorption of water-soluble organic carbon aerosols in the outflow from northern China. *Atmos. Chem. Phys.* **2014**, *14*, 1413−1422.
(7) Bergin, M. H.; Tripathi, S. N.; Jai Devi, J.; Gupta, T.; Mckenzie, M.; Rana, K. S.; Shafer, M. M.; Villalobos, A. M.; Schauer, J. J. The discoloration of the Taj Mahal due to particulate carbon and dust deposition. *Environ. Sci. Technol.* **2015**, *49*, 808−812.
(8) Jo, D. S.; Park, R. J.; Lee, S.; Kim, S.-W.; Zhang, X. A global simulation of brown carbon: implications for photochemistry and direct radiative effect. *Atmos. Chem. Phys.* **2016**, *16*, 3413−3432.
(9) Updyke, K. M.; Nguyen, T. B.; Nizkorodov, S. A. Formation of brown carbon via reactions of ammonia with secondary organic aerosols from biogenic and anthropogenic precursors. *Atmos. Environ.* **2012**, *63*, 22−31.
(10) Shen, Z.; Zhang, Q.; Cao, J.; Zhang, L.; Lei, Y.; Huang, Y.; Huang, R.-J.; Gao, J.; Zhao, Z.; Zhu, C.; Yin, X.; Zheng, C.; Xu, H.; Liu, S. Optical properties and possible sources of brown carbon in $PM_{2.5}$ over Xi'an, China. *Atmos. Environ.* **2017**, *150*, 322−330.
(11) Nakayama, T.; Sato, K.; Matsumi, Y.; Imamura, T.; Yamazaki, A.; Uchiyama, A. Wavelength and NO_x dependent complex refractive index of SOAs generated from the photooxidation of toluene. *Atmos. Chem. Phys.* **2013**, *13*, 531−545.
(12) Lin, P.; Liu, J.; Shilling, J. E.; Kathmann, S.; Laskin, J.; Laskin, A. Molecular characterization of brown carbon (BrC) chromophores in secondary organic aerosol generated from photo-oxidation of toluene. *Phys. Chem. Chem. Phys.* **2015**, *17*, 23312−23325.
(13) Xie, M.; Chen, X.; Hays, M. D.; Lewandowski, M.; Offenberg, J.; Kleindienst, T. E.; Holder, A. L. Light absorption of secondary organic aerosol: Composition and contribution of nitroaromatic compounds. *Environ. Sci. Technol.* **2017**, *51*, 11607−11616.
(14) Bond, T. C.; Doherty, S. J.; Fahey, D.; Forster, P.; Berntsen, T.; DeAngelo, B.; Flanner, M.; Ghan, S.; Kaercher, B.; Koch, D.; et al. Bounding the role of black carbon in the climate system: A scientific assessment. *J. Geophys. Res. Atmos.* **2013**, *118*, 5380−5552.
(15) Weingartner, E.; Saathoff, H.; Schnaiter, M.; Streit, N.; Bitnar, B.; Baltensperger, U. Absorption of light by soot particles: determination of the absorption coefficient by means of aethalometers. *J. Aerosol Sci.* **2003**, *34*, 1445−1463.
(16) Lack, D. A.; Bahreni, R.; Langridge, J. M.; Gilman, J. B.; Middlebrook, A. M. Brown carbon absorption linked to organic mass tracers in biomass burning particles. *Atmos. Chem. Phys.* **2013**, *13*, 2415−2422.
(17) Massabò, D.; Caponi, L.; Bernardoni, V.; Bove, M. C.; Brotto, P.; Calzolai, G.; Cassola, F.; Chiari, M.; Fedi, M. E.; Fermo, P.; et al.

Multi-wavelength optical determination of black and brown carbon in atmospheric aerosols. *Atmos. Environ.* **2015**, *108*, 1−12.
(18) Sun, H.; Biedermann, L.; Bond, T. C. Color of brown carbon: A model for ultraviolet and visible light absorption by organic carbon aerosol. *Geophys. Res. Lett.* **2007**, *34*, L17813.
(19) Chen, Y.; Bond, T. C. Light absorption by organic carbon from wood combustion. *Atmos. Chem. Phys.* **2010**, *10*, 1773−1787.
(20) Phillips, S. M.; Smith, G. D. Light absorption by charge transfer complexes in brown carbon aerosols. *Environ. Sci. Technol. Lett.* **2014**, *1*, 382−386.
(21) Hoffer, A.; Gelencsér, A.; Guyon, P.; Kiss, G.; Schmid, O.; Frank, G. P.; Artaxo, P.; Andreae, M. O. Optical properties of humic-like substances (HULIS) in biomass-burning aerosols. *Atmos. Chem. Phys.* **2006**, *6*, 3563−3570.
(22) Kirchstetter, T. W.; Thatcher, T. L. Contribution of organic carbon to wood smoke particulate matter absorption of solar radiation. *Atmos. Chem. Phys.* **2012**, *12*, 6067−6072.
(23) Lack, D. A.; Langridge, J. M.; Bahreini, R.; Cappa, C. D.; Middlebrook, A. M.; Schwarz, J. P. Brown carbon and internal mixing in biomass burning particles. *Proc. Natl. Acad. Sci. U. S. A.* **2012**, *109*, 14802−14807.
(24) Shamjad, P. M.; Tripathi, S. N.; Thamban, N. M.; Vreeland, H. Refractive index and absorption attribution of highly absorbing brown carbon aerosols from an urban Indian city-Kanpur. *Sci. Rep.* **2016**, *6*, 37735.
(25) Mok, J.; Krotkov, N. A.; Arola, A.; Torres, O.; Jethva, H.; Andrade, M.; Labow, G.; Eck, T. F.; Li, Z.; Dickerson, R. R.; Stenchikov, G. L.; Osipov, S.; Ren, X. Impacts of brown carbon from biomass burning on surface UV and ozone photochemistry in the Amazon Basin. *Sci. Rep.* **2016**, *6*, 36940.
(26) Feng, Y.; Ramanathan, V.; Kotamarthi, V. Brown carbon: a significant atmospheric absorber of solar radiation? *Atmos. Chem. Phys.* **2013**, *13*, 8607−8621.
(27) Kirchstetter, T. W.; Novakov, T.; Hobbs, P. V. Evidence that the spectral dependence of light absorption by aerosols is affected by organic carbon. *J. Geophys. Res. Atmos.* **2004**, *109*, 1−12.
(28) Hecobian, A.; Zhang, X.; Zheng, M.; Frank, N.; Edgerton, E. S.; Weber, R. Water-soluble organic aerosol material and the light-absorption characteristics of aqueous extracts measured over the Southeastern United States. *Atmos. Chem. Phys.* **2010**, *10*, 5965−5977.
(29) Zhang, X.; Lin, Y. H.; Surratt, J. D.; Zotter, P.; Prevot, A. S. H.; Weber, R. J. Light-absorbing soluble organic aerosol in Los Angeles and Atlanta: A contrast in secondary organic aerosol. *Geophys. Res. Lett.* **2011**, *38*, L21810.
(30) Cheng, Y.; He, K.-B.; Du, Z.-Y.; Engling, G.; Liu, J.-M.; Ma, Y.-L.; Zheng, M.; Weber, R. J. The characteristics of brown carbon aerosol during winter in Beijing. *Atmos. Environ.* **2016**, *127*, 355−364.
(31) Liu, J.; Bergin, M.; Guo, H.; King, L.; Kotra, N.; Edgerton, E.; Weber, R. J. Size-resolved measurements of brown carbon in water and methanol extracts and estimates of their contribution to ambient fine-particle light absorption. *Atmos. Chem. Phys.* **2013**, *13*, 12389−12404.
(32) Kim, H.; Kim, J. Y.; Jin, H. C.; Lee, J. Y.; Lee, S. P. Seasonal variations in the light-absorbing properties of water-soluble and insoluble organic aerosols in Seoul, Korea. *Atmos. Environ.* **2016**, *129*, 234−242.
(33) Paatero, P.; Tapper, U. Positive Matrix Factorization: A non-negative factor model with optimal utilization of error stimates od data values. *Environmetrics* **1994**, *5*, 111−126.
(34) Sun, Y.; Zhang, Q.; Zheng, M.; Ding, X.; Edgerton, E. S.; Wang, X. Characterization and source apportionment of water-soluble organic matter in atmospheric fine particles ($PM_{2.5}$) with high-resolution aerosol mass spectrometry and GC-MS. *Environ. Sci. Technol.* **2011**, *45*, 4854−4861.
(35) Washenfelder, R. A.; Attwood, A. R.; Brock, C. A.; Guo, H.; Xu, L.; Weber, R. J.; Ng, N. L.; Allen, H. M.; Ayres, B. R.; Baumann, K.; et al. Biomass burning dominates brown carbon absorption in the rural southeastern United States. *Geophys. Res. Lett.* **2015**, *42*, 653−664.
(36) Elser, M.; Huang, R.-J.; Wolf, R.; Slowik, J. G.; Wang, Q.; Canonaco, F.; Li, G.; Bozzetti, C.; Daellenbach, K. R.; Huang, Y.; et al. New insights into $PM_{2.5}$ chemical composition and sources in two major cities in China during extreme haze events using aerosol mass spectrometry. *Atmos. Chem. Phys.* **2016**, *16*, 3207−3225.
(37) Daellenbach, K. R.; Bozzetti, C.; Krepelová, A.; Canonaco, F.; Wolf, R.; Zotter, P.; Fermo, P.; Crippa, M.; Slowik, J. G.; Sosedova, Y.; et al. Characterization and source apportionment of organic aerosol using offline aerosol mass spectrometry. *Atmos. Meas. Tech.* **2016**, *9*, 23−39.
(38) Daellenbach, K. R.; Stefenelli, G.; Bozzetti, C.; Vlachou, A.; Fermo, P.; Gonzalez, R.; Piazzalunga, A.; Colombi, C.; Canonaco, F.; Hueglin, C.; et al. Long-term chemical analysis and organic aerosol source apportionment at nine sites in central Europe: source identification and uncertainty assessment. *Atmos. Chem. Phys.* **2017**, *17*, 13265−13282.
(39) Bozzetti, C.; Sosedova, Y.; Xiao, M.; Daellenbach, K. R.; Ulevicius, V.; Dudoitis, V.; Mordas, G.; Bycenkiene, S.; Plauskaite, K.; Vlachou, A.; et al. Argon offline-AMS source apportionment of organic aerosol over yearly cycles for an urban, rural, and marine site in northern Europe. *Atmos. Chem. Phys.* **2017**, *17*, 117−141.
(40) Laskin, A.; Laskin, J.; Nizkorodov, S. A. Chemistry of atmospheric brown carbon. *Chem. Rev.* **2015**, *115*, 4335−4382.
(41) Yang, M.; Howell, S. G.; Zhuang, J.; Huebert, B. J. Attribution of aerosol light absorption to black carbon, brown carbon, and dust in China−interpretations of atmospheric measurements during EAST-AIRE. *Atmos. Chem. Phys.* **2009**, *9*, 2035−2050.
(42) Paatero, P. The multilinear engine: A table-driven, least squares program for solving multilinear problems, including the n-way parallel factor analysis model. *J. Comput. Graph. Stat.* **1999**, *8*, 854−888.
(43) Canonaco, F.; Crippa, M.; Slowik, J. G.; Baltensperger, U.; Prévôt, A. S. H. SoFi, an IGOR-based interface for the efficient use of the generalized multilinear engine (ME-2) for the source apportionment: ME-2 application to aerosol mass spectrometer data. *Atmos. Meas. Tech.* **2013**, *6*, 3649−3661.
(44) Paatero, P.; Eberly, S.; Brown, S. G.; Norris, G. A. Methods for estimating uncertainty in factor analytic solutions. *Atmos. Meas. Tech.* **2014**, *7*, 781−797.
(45) Lundstedt, S.; White, P. A.; Lemieux, C. L.; Lynes, K. D.; Lambert, L. B.; Oberg, L.; Haglund, P.; Tysklind, M. Sources, fate, and toxic hazards of oxygenated polycyclic aromatic hydrocarbons (PAHs) at PAH-contaminated sites. *Ambio.* **2007**, *36*, 475−485.
(46) Duarte, R. M. B. O.; Santos, E. B. H.; Pio, C. A.; Duarte, A. C. Comparison of structural features of water-soluble organic matter from atmospheric aerosols with those of aquatic humic substances. *Atmos. Environ.* **2007**, *41*, 8100−8113.
(47) Sandradewi, J.; Prévôt, A. S. H.; Weingartner, E.; Schmidhauser, R.; Gysel, M.; Baltensperger, U. A study of wood burning and traffic aerosols in an Alpine valley using a multi-wavelength Aethalometer. *Atmos. Environ.* **2008**, *42*, 101−112.
(48) Zotter, P.; Ciobanu, V. G.; Zhang, Y. L.; El-Haddad, I.; Macchia, M.; Daellenbach, K. R.; Salazar, G. A.; Huang, R.-J.; Wacker, L.; Hueglin, C.; et al. Radiocarbon analysis of elemental and organic carbon in Switzerland during winter-smog episodes from 2008 to 2012-Part 1: Source apportionment and spatial variability. *Atmos. Chem. Phys.* **2014**, *14*, 13551−13570.
(49) Lin, P.; Bluvshtein, N.; Rudich, Y.; Nizkorodov, S. A.; Laskin, J.; Laskin, A. Molecular chemistry of atmospheric brown carbon inferred from a nationwide biomass burning event. *Environ. Sci. Technol.* **2017**, *51*, 11561−11570.
(50) Hu, Z.; Kang, S.; Li, C.; Yan, F.; Chen, P.; Gao, S.; Wang, Z.; Zhang, Y.; Sillanpää, M. Light absorption of biomass burning and vehicle emission-sourced carbonaceous aerosols of the Tibetan Plateau. *Environ. Sci. Pollut. Res.* **2017**, *24*, 15369−15378.
(51) Olson, M. R.; Victoria Garcia, M.; Robinson, M. A.; Van Rooy, P.; Dietenberger, M. A.; Bergin, M.; Schauer, J. J. Investigation of black and brown carbon multiple-wavelength-dependent light absorption from biomass and fossil fuel combustion source emissions. *J. Geophys. Re. Atmos.* **2015**, *120*, 6682−6697.
(52) Pandey, A.; Pervez, S.; Chakrabarty, R. J. Filter-based measurements of UV−vis mass absorption cross sections of organic

DOI: 10.1021/acs.estlett.8b00118
Environ. Sci. Technol. Lett. 2018, 5, 302−308

carbon aerosol from residential biomass combustion: Preliminary findings and sources of uncertainty. *J. Quant. Spectrosc. Radiat. Transf.* **2016**, *182*, 296−304.
(53) Kumar, N. K.; Corbin, J. C.; Bruns, E. A.; Gysel, M.; Massabó, D.; Slowik, J. G.; Drinovec, L.; Močnik, G.; Prati, P.; Vlachou, A. Production of particulate brown carbon during atmospheric aging of wood-burning emissions. *Atmos. Chem. Phys. Discuss.* 2018. https://doi.org/10.5194/acp-2018-159
(54) Yan, C.; Zheng, M.; Bosch, C.; Andersson, A.; Desyaterik, Y.; Sullivan, A. P.; Collett, J. L.; Zhao, B.; Wang, S.; He, K.; Gustafsson, Ö. Important fossil source contribution to brown carbon in Beijing during winter. *Sci. Rep.* **2017**, *7*, 43182.
(55) Alexander, D. T. L.; Crozier, P. A.; Anderson, J. R. Brown carbon spheres in East Asian outflow and their optical properties. *Science* **2008**, *321*, 833−836.
(56) Dinar, E.; Abo Riziq, A.; Spindler, C.; Erlick, C.; Kiss, G.; Rudich, Y. The complex refractive index of atmospheric and model humic-like substances (HULIS) retrieved by a cavity ring down aerosol spectrometer (CRD-AS). *Faraday Discuss.* **2008**, *137*, 279−295.
(57) Chakrabarty, R. K.; Pervez, S.; Chow, J. C.; Watson, J. G.; Dewangan, S.; Robles, J.; Tian, G. Funeral pyres in South Asia: Brown carbon aerosol emissions and climate impacts. *Environ. Sci. Technol. Lett.* **2014**, *1*, 44−48.
(58) Bruns, E. A.; El Haddad, I.; Slowik, J. G.; Kilic, D.; Klein, F.; Baltensperger, U.; Prévôt, A. S. H. Identification of significant precursor gases of secondary organic aerosols from residential wood combustion. *Sci. Rep.* **2016**, *6*, 27881.
(59) Vlachou, A.; Daellenbach, K. R.; Bozzetti, C.; Chazeau, B.; Salazar, G. A.; Szidat, S.; Jaffrezo, J.-L.; Hueglin, C.; Baltensperger, U.; El Haddad, I.; Prévôt, A. S. H. Advanced source apportionment of carbonaceous aerosols by coupling offline AMS and radiocarbon size segregated measurements over a nearly two-year period. *Atmos. Chem. Phys.* **2018**, *18*, 6187−6206.
(60) Sumlin, B. J.; Pandey, A.; Walker, M. J.; Pattison, R. S.; Williams, B. J.; Chakrabarty, R. K. Atmospheric photooxidation diminishes light absorption by primary brown carbon aerosol from biomass burning. *Environ. Sci. Technol. Lett.* **2017**, *4*, 540−545.
(61) Romonosky, D. E.; Ali, N. N.; Saiduddin, M. N.; Wu, M.; Lee, H. J.; Aiona, P. K.; Nizkorodov, S. A. Effective absorption cross sections and photolysis rates of anthropogenic and biogenic secondary organic aerosols. *Atmos. Environ.* **2016**, *130*, 172−179.
(62) Lewis, A. C.; Evans, M. J.; Hopkins, J. R.; Punjabi, S.; Read, K. A.; Purvis, R. M.; Andrews, S. J.; Moller, S. J.; Carpenter, L. J.; Lee, J. D.; Rickard, A. R.; Palmer, P. I.; Parrington, M. The influence of biomass burning on the global distribution of selected non-methane organic compounds. *Atmos. Chem. Phys.* **2013**, *13*, 851−867.
(63) Chen, J.; Li, C.; Ristovski, Z.; Milic, A.; Gu, Y.; Islam, M. S.; Wang, S.; Hao, J.; Zhang, H.; He, C.; et al. A review of biomass burning: Emissions and impacts on air quality, health and climate in China. *Sci. Total Environ.* **2017**, *579*, 1000−1034.
(64) Daellenbach, K. R.; El-Haddad, I.; Karvonen, L.; Vlachou, A.; Corbin, J. C.; Slowik, J. G.; Heringa, M. F.; Bruns, E. A.; Luedin, S. M.; Jaffrezo, J.-L.; et al. Insights into organic-aerosol sources via a novel laser-desorption/ionization mass spectrometry technique applied to one year of PM_{10} samples from nine sites in central Europe. *Atmos. Chem. Phys.* **2018**, *18*, 2155−2174.
(65) Zhang, H.; Yee, L. D.; Lee, B. H.; Curtis, M. P.; Worton, D. R.; Isaacman-VanWertz, G.; Offenberg, J. H.; Lewandowski, M.; Kleindienst, T. E.; Beaver, M. R.; et al. Monoterpenes are the largest source of summertime organic aerosol in the southeastern United States. *Proc. Natl. Acad. Sci. U. S. A.* **2018**, *115*, 2038−2043.
(66) Kirillova, E. N.; Andersson, A.; Tiwari, S.; Srivastava, A. K.; Bisht, D. S.; Gustafsson, Ö. Water-soluble organic carbon aerosols during a full New Delhi winter: Isotope-based source apportionment and optical properties. *J. Geophys. Res. Atmos.* **2014**, *119*, 3476−3485.
(67) Hoffer, A.; Tóth, A.; Nyiro-Kósa, I.; Pósfai, M.; Gelencsér, A. Light absorption properties of laboratory-generated tar ball particles. *Atmos. Chem. Phys.* **2016**, *16*, 239−246.
(68) Ciarelli, G.; Aksoyoglu, S.; El Haddad, I.; Bruns, E. A.; Crippa, M.; Poulain, L.; Äijälä, M.; Carbone, S.; Freney, E.; O'Dowd, C.; Baltensperger, U.; Prévôt, A. S. H. Modelling winter organic aerosol at the European scale with CAMx: evaluation and source apportionment with a VBS parameterization based on novel wood burning smog chamber experiments. *Atmos. Chem. Phys.* **2017**, *17*, 7653−7669.

DOI: 10.1021/acs.estlett.8b00118
Environ. Sci. Technol. Lett. 2018, 5, 302−308